

Cover page

Design of the RF ion source for the ITER NBI

D.Marcuzzi, P.Agostinetti, M.Dalla Palma, H.D.Falter*, B.Heinemann*, R.Riedl*

Consorzio RFX, Euratom-ENEA Association, Corso Stati Uniti 4, I-35127 Padova, Italy

* Max-Planck-Institut für Plasmaphysik, D-85748 Garching, Germany

Corresponding author:

Dr Diego Marcuzzi
Consorzio RFX
Associazione EURATOM-ENEA sulla fusione
Corso Stati Uniti, 4
35127 Padova, ITALY
tel : +39/049/8295923
fax: +39/049/8700718
e-mail: diego.marcuzzi@igi. cnr.it

Design of the RF ion source for the ITER NBI

D.Marcuzzi, P.Agostinetti, M.Dalla Palma, H.D.Falter*, B.Heinemann*, R.Riedl*

Consorzio RFX, Euratom-ENEA Association, Corso Stati Uniti 4, I-35127 Padova, Italy

* Max-Planck-Institut für Plasmaphysik, D-85748 Garching, Germany

Abstract

A Radio Frequency (RF) driven negative ion source has been designed for the ITER neutral beam injectors, as an alternative to the traditional arc driven solution.

The main advantage of this technology is to avoid the presence of the filaments, that require periodic maintenance and consequently frequent shutdowns.

The requirements for the ion source of the ITER NBI are to provide a uniform flux of D⁻/H⁻ to the plasma grid of the accelerator that will result in a beam current of 40 A at 1 MeV. The present specification is for a filling pressure of 0.3 Pa. The ion source needs to provide 20/28 mA/cm² D⁻/H⁻ current density across the 0.58 x 1.54 m² aperture array for 3600 s.

The source, consisting of a main chamber facing the plasma grid, of eight RF drivers and the auxiliary systems for power transfer, cooling and diagnostic purposes, is housed in the same quasi-cylindrical structure that supports the arc driven solution.

Specific electric and hydraulic circuits have been designed and verified.

In the paper the analyses performed for the design of the components are presented in detail.

Keywords : ITER, NBI, Ion source, Radio Frequency

1. Introduction

In the frame of the EFDA task, regarding the design of the ITER Neutral Beam Injector (NBI), one of the main objectives was to develop the study of a Radio Frequency (RF) driven ion source, as an alternative to the reference arc driven ion source [1].

The reason is mainly the advantage of avoiding the presence of power filaments, that require periodic maintenance and consequently periodic shutdowns [2].

The conceptual scheme of a RF ion source [3] consists of a main case that acts as an expansion region for the plasma generated in the drivers, where the power is input. The negative ions created next to the plasma grid are extracted similarly to the arc driven source.

The main performances requested for the ion source of the ITER NBI are [1]: 40 A accelerated beam current, 20/28 mA/cm² D⁻/H⁻ current density at 1 MeV, 0.3 Pa source pressure, 3600 s pulse length, 1.5 x 0.6 m² cross section with a total aperture area on the plasma grid of 0.2 m².

2. Design description

2.1 General description

The RF ion source for the ITER NBI has been designed on the basis of the existing smaller size sources being operated by the Max-Planck-Institut für Plasmaphysik in Garching [4].

Isometric views of the designed RF ion source are reported in figure 1.

The source features eight drivers (four rows of two drivers) where the RF power is input; the drivers are connected to the source case, an open box that faces the plasma grid in the beam source assembly. The $1760 \times 860 \text{ mm}^2$ source case cross section dimensions exceed the plasma grid aperture array dimensions, $1500 \times 575 \text{ mm}^2$, in order to minimise beam border non-homogeneities.

The design of the source also includes the electric circuit for power input and the cooling circuits for heated components, as described in sect.2.4 and 2.5.

Ports are foreseen on the back cover of the drivers and on the source case surface, in order to allow the connection of the auxiliary systems and the diagnostic accesses.

2.2 Drivers

The drivers are the components where the power is transferred into the RF ion source and the plasma is generated.

The driver is a cylindrical chamber with about 250 mm diameter, as shown in fig.2, directly connected to the source case, and consisting of a lateral wall in alumina and a stainless steel back cover.

The following items are fixed/connected onto the cover: auxiliary systems on the outside (gas injection, starter filament, Faraday shield cooling, diagnostics), Faraday Shield and permanent magnets for plasma confinement on the inside.

The actively cooled Faraday shield, made of electrodeposited copper, is placed inside the driver in order to protect the alumina driver case from the heat load of the plasma.

The RF power is applied to a tubular copper coil wound on the outside of the driver case. Insulation is provided by an external layer of alumina, plasma sprayed on the

outside of the coil, the vacuum and properly shaped and insulated fixing systems that keep the proper pitch between coil turns.

2.3 Source case

The source case is the main body of the source, where the plasma generated in the drivers flows into. The case is a box, open on the side facing the plasma grid in the beam source assembly, and consisting of a rear plate (called drivers plate, as drivers are fixed onto it) a lateral wall in stainless steel and a front plate, as shown in figure 1.

A large body of evidence suggests that the majority of the extracted negative ions in this type of ion source are created on the plasma grid; this phenomenon is facilitated by the injection of caesium inside the source, which acts as a catalyst for the negative ions production.

An electrodeposited layer of copper (1 mm thickness) on the internal surface contributes to the uniformity of temperature distribution on the case: this is needed to avoid cold spots (under 40°C) on the internal surface of the source case that would be detrimental of the caesium behaviour [3].

Two caesium ovens are foreseen connected on the outside of the drivers plate for controlled injection of caesium.

Permanent magnets, which create the magnetic field for enhancing the plasma confinement, are positioned in dedicated grooves on the outside of the drivers plate and in special elements fixed on outside of the lateral wall.

2.4 Electric circuits

Inside the drivers the input power coming from the power supply is transferred by the RF coils to the injected gas, that ionizes and generates the plasma.

Four identical circuits are connected in parallel [5], as shown in figure 3: each horizontal pair of drivers is put in series with a variable capacitor (C2); a fixed capacitor (C1) is connected in parallel to the previous elements.

The C2 variable capacitor allows, in a preliminary operational phase at low voltage and radiation, to remotely adjust the capacitance by means of an electric actuator.

Subsequently, the tuning of the circuit will be done by controlling the power generator frequency.

2.5 Hydraulic circuit

Three independent hydraulic circuits are foreseen for the following components: RF coils, Faraday shields (FS) and source case.

The need to control the source case temperature for optimal management of the caesium [3] and the large heat load on the FS justifies the independence of the circuits.

Eighteen cooling channels in parallel are embedded in the FS lateral wall, in the space between the cuts foreseen to prevent circulation of eddy currents, as shown in figure 4.

Inlet and outlet channels are embedded at different levels in the FS back plate.

The external cooling circuit for the Faraday shields consists in an inlet and an outlet vertical manifold with the eight connections in parallel to the back of the drivers.

The tubular shape of the RF coils allows to combine the hydraulic and electric circuits around the drivers: cooling water flows inside the tube (4 mm internal diameter), to evacuate the heat generated by the current.

The independence of the four electric circuits requires ceramic breaks between the inlet/outlet main water manifolds and each series of two drivers.

The heat load on the source case is exhausted by means of three cooling circuit in parallel, that use the same vertical inlet and outlet manifolds, as shown in fig.5.

One circuit cools the lateral wall: the water enters from the front plate in two different positions, then passes through a tangential groove, flows into 204 channels drilled in the thickness of the side walls parallel to the beam direction and exits from the drivers plate in a similar way to the entrance.

The drivers plate is cooled by two couples of channels machined on the internal surface and closed by subsequent electro-deposition of 1 mm layer of copper on the whole surface, as shown in fig.5.

The water inlets and outlets are placed on the back of the drivers plate.

2.6 Beam source assembly and integration in the injector

The main goal regarding the integration of the RF source in the injector and in particular in the beam source assembly was to replace the arc driven ion source with the RF driven ion source while causing the minimum impact on the rest of the beam source assembly and on adjacent components.

The configuration featuring the RF ion source with only the SINGle GAP (SINGAP) accelerator has been considered in detail, leaving aside the adaptation with the Multi Aperture Multi Grid (MAMuG) reference solution. The final design requires no modification of the SINGAP accelerator part adjacent to the ion source, called extractor [6,7].

The external side of the structure that supports the ion source hasn't been changed, therefore the support and positioning system for the whole beam source assembly, in SINGAP configuration, is valid for both the RF driven ion source and the reference ion source, as it's connected on the outside of this structure [3,6,7].

The beam source assembly (RF ion source + SINGAP extractor assembly) is shown in figure 6: the support and positioning system has been hidden in order to view the source. Due to differences in shape, dimensions and functional parameters of the RF driven ion source and the reference ion source, few other components had minor revisions with respect to the arc driven solution, such as magnetic shield, bias and plasma grid (PG) bus bars.

3. Design analyses

3.1 Criteria

The RF ion source hydraulic circuits should be considered equivalent to the other in-vessel components of ITER, hence the design criteria contained in the ITER Structural Design Criteria for In-vessel Components [8] have been used.

A preliminary power deposition balance was estimated on the basis of measurements taken on IPP test beds [9]: the considered loads for the analysis are 800 kW total input power, that result in 400 kW on the FS, 250 kW on the source case, few tens on the RF electric circuit, the rest on plasma grid and other components (drivers back cover, for instance), apart from the power absorbed by the plasma itself.

Analytical calculations have been carried out to assess the overall behaviour of the cooling circuits, together with a preliminary sensitivity analysis for the main parameters.

A Finite Element (FE) model was then developed for the FS, being recognised as the most critical issue and the least coherent to one-dimensional models.

Coolant inlet temperature was always set to 20°C.

Water velocity should be kept under 6 m/s, water maximum temperature within values that don't influence electrical conductivity (<60-70°C), while stress distribution should be preliminarily kept under 107 MPa (yield stress of annealed copper @ 300°C after cyclic hardening [10]), but further detailed fatigue verification will be needed.

3.2 Preliminary analytical evaluations

The heat transfer process inside the cooling channels is ruled by forced convection in single phase flow.

Well known formulas [8,11] have been adopted for the evaluation of relevant parameters such as heat transfer coefficient (Sieder-Tate) and pressure drop (Colebrook-White).

The overall behaviour of the cooling circuits has been evaluated, in terms of flow rate and temperature rise as reported in table 1.

Two RF coils have been considered in series, as explained in section 2.5, with a total length larger than 10 m. The water velocity was varied in the range $2 \div 4$ m/s, in order to find a compromise between the pressure drop and the water temperature rise.

Evaluations still need to be carried out to assess the allowable variation of water resistivity with temperature: if necessary the 8 coils could be put all in parallel, in order to limit the temperature rise.

For the source case, preliminary calculations were carried out on the lateral wall and drivers plate cooling circuits. The analyses show acceptable values for the lateral wall

that should provide uniform temperature distribution, but the first results for the drivers plate indicate the need to improve the cooling in the drivers plate, e.g. doubling the loops from 4 to 8.

The analyses on the FS indicate a large temperature rise with the $3 \times 1 \text{ mm}^2$ channel cross-section, and a substantial reduction with an enlarged solution of $4 \times 1.4 \text{ mm}^2$.

The complex shape of the FS cooling loop means that a more detailed analysis is to be carried out, in order to verify the three dimensional temperature and stress distributions, as described in the next section. It is to be noted that no detail information on power distribution was available for these preliminary analyses, hence a uniform power density distribution on the internal cylindrical wall was adopted to take account of the effects of plasma interaction and eddy currents.

3.3 FE thermo-mechanical analyses of the Faraday shield

The full FS was modelled with fluid one-dimensional elements to account for the water properties, surface elements on the channel wall to calculate the convection heat transfer and solid elements for the copper thermal and structural properties.

The properties of fully annealed oxygen free high conductivity copper (OFHC-Cu), temperature dependent, have been used for all the analyses.

A uniform power density was applied on the internal cylindrical wall of the Faraday shield.

Fluid-thermal and thermo-structural analyses were carried out to investigate the effect of various parameters (heat flux, water flow, model geometry) on the Faraday shield behaviour, in terms of temperature of the water and of the cooling channels walls, temperature and stresses in the copper.

In figure 7 and 8 the temperature and stress distributions in the copper are shown for the reference configuration ($3 \times 1 \text{ mm}^2$ channel cross section and 0.25 kg/s water flow).

In table 2 the main results of the water flow sensitivity analysis with high heat flux (50 kW) are reported.

The numerical calculations confirm that the FS is the most critical component of the RF source from the thermo-hydraulic point of view: the enlargement of the cooling channels is highly advisable, and it is recommended to perform more accurate measurements of the total power deposited in currently operating test beds, as the influence of the heat flux on the temperature rise and on the maximum stress could become critical.

4. Conclusions

The RF source for ITER has been designed with a level of detail comparable with the reference arc driven solution.

The integration in the beam source assembly and the interfaces with the other components of the injector have been positively assessed: the RF ion source fits properly the support structure designed for the arc driven ion source.

An assessment of the RF ion source design has been accomplished, by means of analytical and numerical calculations: detailed analyses were carried out in order to characterize the thermo-mechanical behaviour of the Faraday shield, that was found to be the most critical component.

The maximization of the FS cooling circuit water flow was found necessary to limit the temperature and stress levels in the electrodeposited copper.

The next experimental campaign on IPP test beds (MANITU, for long pulses, and RADI, for scaling factors) will help check the solutions adopted and the analyses done.

5. Acknowledgements

This work, supported by the European Communities under the contracts of Association between EURATOM and ENEA, and between EURATOM and IPP, was carried out within the framework of the European Fusion Development Agreement (EFDA task TW4-THHN-IITF2). The views and opinions expressed herein do not necessarily reflect those of the European Commission.

The authors would like to highlight the valuable contribution by the company Design&Consulting.

References

- [1] ITER Neutral Beam Heating & Current Drive System, Design Description Document (DDD 5.3) N53 DDD 29 01-07-03 R 0.1
- [2] W. Kraus, et al., Development of large RF driven negative ion sources for neutral beam injection, *Fusion-Engineering-and-Design*. Sept. 2003; 66-68: 491-5
- [3] P. Franzen, et al., Status and plans for the development of a RF negative ion source for ITER NBI, *Fusion-Engineering-and-Design*. Nov. 2005; 74: 351-7
- [4] E. Speth et al, Overviews of the RF source development programme at IPP Garching, *Nucl. Fusion* 46 (2006) S220-S238.
- [5] E. Gaio, et al., Studies on the Radio Frequency power supply system for the ITER NB Injector Ion Source, in: proceedings of the 24th SOFT conference (2006)
- [6] S. Peruzzo, G. Anaclerio, S. Dal Bello, M. Dalla Palma, R. Nocentini, P. Zaccaria, Thermal analyses and design review of ITER NBI arc driven ion source, in: proceedings of the 24th SOFT conference (2006)
- [7] P. Agostinetti, M. Dalla Palma, S. Dal Bello, P. Zaccaria, Thermo-mechanical design of the SINGAP accelerator grids for ITER NB Injectors, in: proceedings of the 24th SOFT conference (2006)
- [8] ITER Structural Design Criteria for In-vessel Components (SDC-IC), G 74 MA 8 R0.1, July 2004
- [9] W. Kraus, M. Fröschle, Private communication
- [10] ITER Material Properties Handbook, G 74 MA 16, ITER-AK01-2424
- [11] John H. Lienhard, *A Heat Transfer Handbook*, Third Edition, Cambridge Massachusetts

List of figures / tables

Fig.1 Isometric views of the RF ion source – rear and front side

Fig.2 Isometric views of the driver assembly – rear and front side

Fig.3 Electric circuit for the RF source – full scheme and isometric view

Fig.4 Isometric view of the Faraday shield

Fig.5 Source case cooling circuits : the cooling water flows into a header channel on the downstream plate (blue arrows), then through the side walls (pink arrows) to the header on the drivers plate and out (red arrow)

Fig.6 Isometric view of the NBI beam source, in the RF driven – SINGAP configuration

Fig.7 Temperature distribution in the FS [$^{\circ}\text{C}$], with 50 kW heat load and 0.25 kg/s mass flow rate

Fig.8 Von Mises stress [Pa] distribution in the FS, with 50 kW heat load and 0.25 kg/s mass flow (deformed shape amplified x200)

Table 1 Main results of the preliminary analytical evaluations

Table 2 Results of the water flow sensitivity analysis (total heat load = 50 kW)

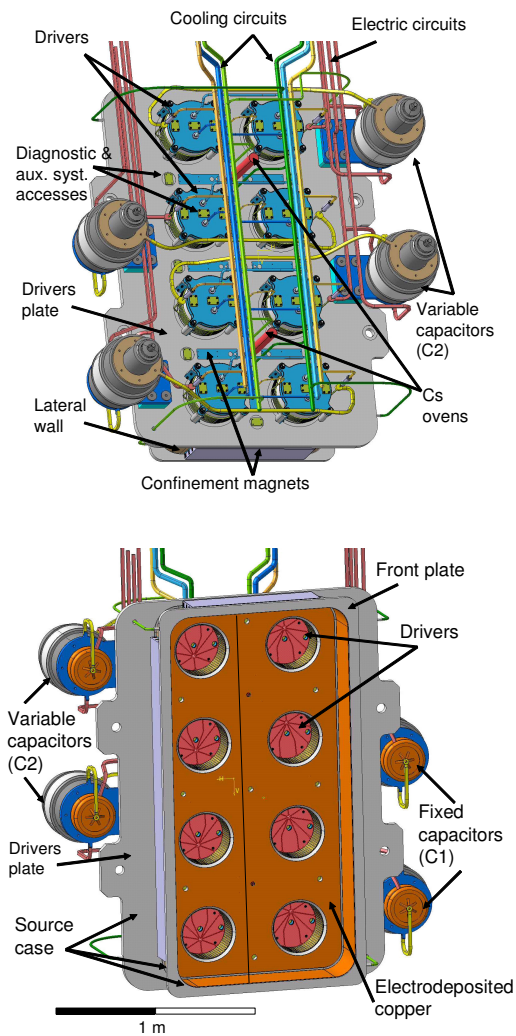


Fig.1 Isometric view of the RF ion source – (a) rear and (b) front side

1/4pp

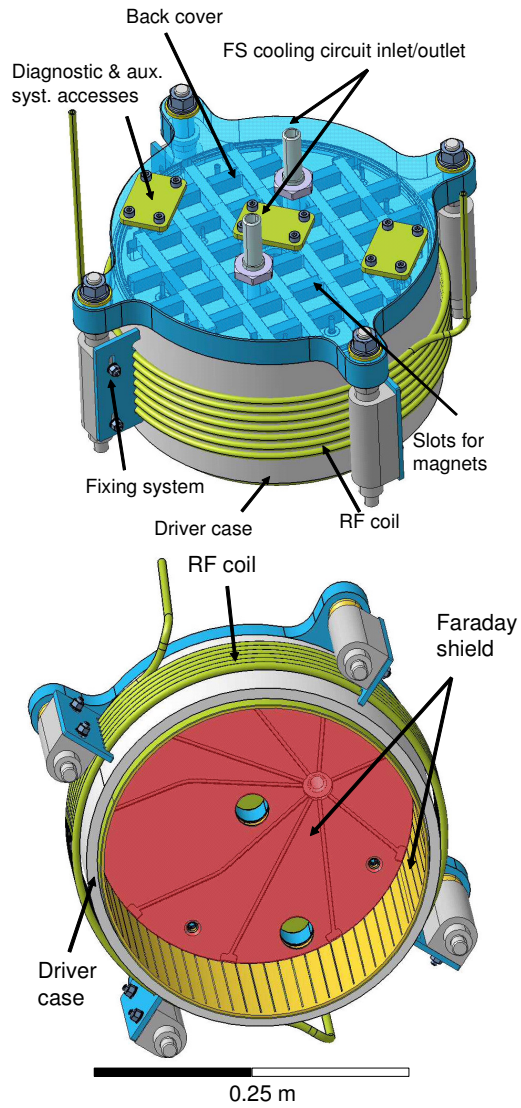


Fig.2 Isometric view of the driver assembly – (a) rear and (b) front side

1/4pp

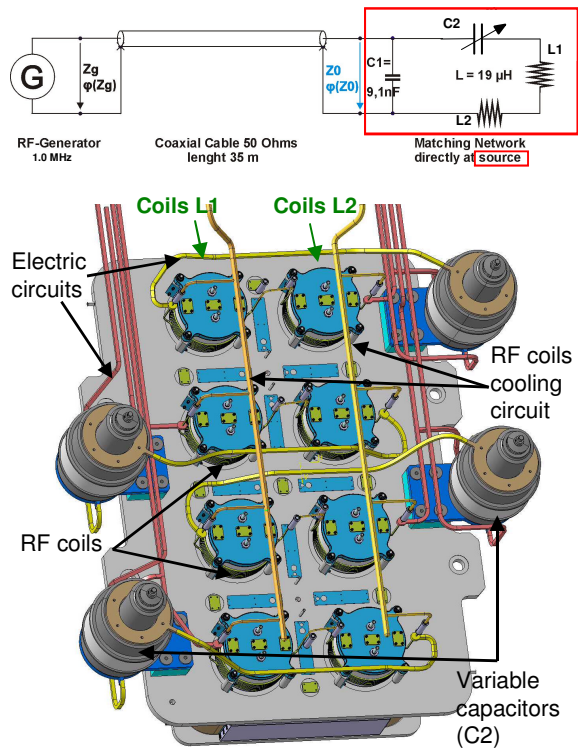


Fig.3 Electric circuit for the RF source – full scheme and isometric view

1/4pp

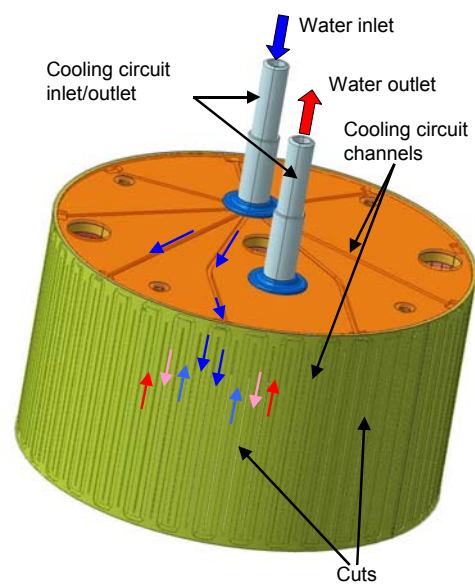


Fig.4 Isometric view of the Faraday shield

1/6 pp

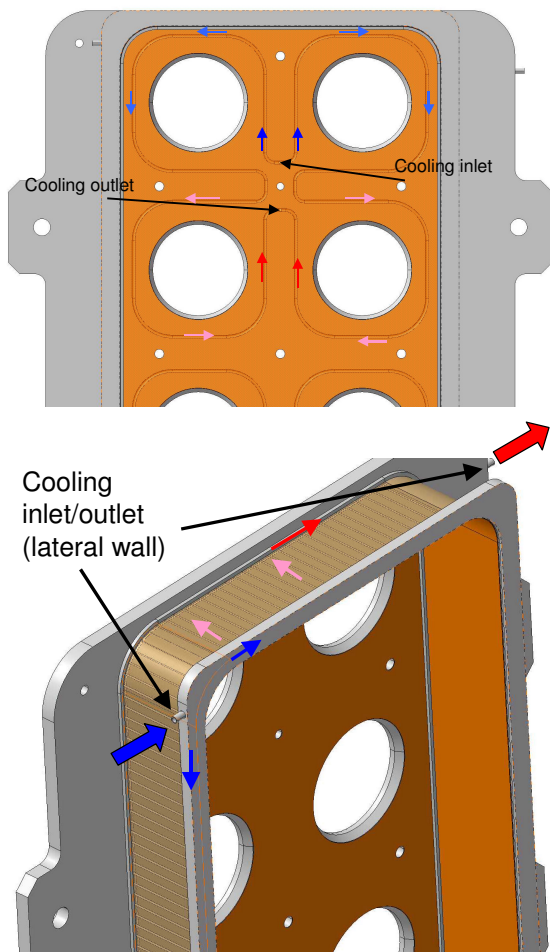


Fig.5 Source case cooling circuits : the cooling water flows into a header channel on the downstream flange (blue arrows), then through the side walls (pink arrows) to the header on the rear flange and out (red arrow)

1/4 pp

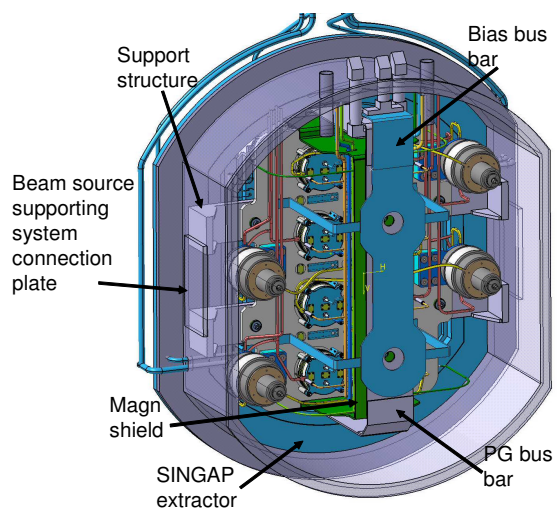


Fig.6 Isometric view of the NBI beam source, in the RF driven – SINGAP configuration. The external support system of the whole beam source is not shown.

1/6 pp

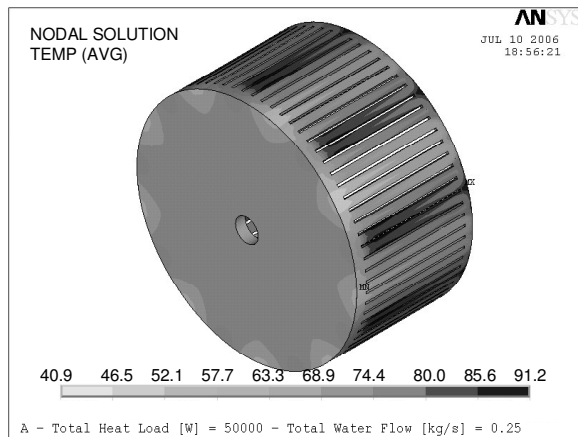


Fig.7 Temperature distribution on copper [°C], with 50 kW heat load and 0.25 kg/s mass flow

1/6 pp

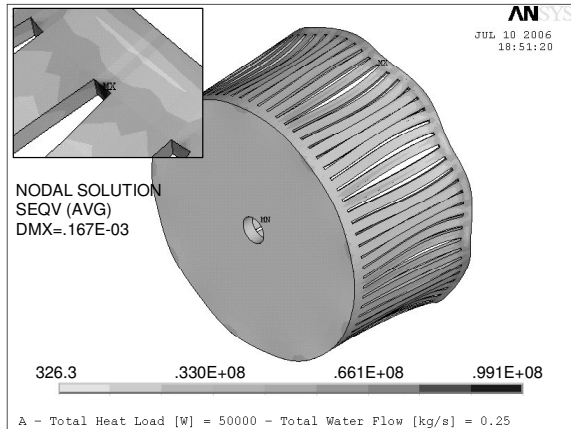


Fig.8 Von Mises stress [Pa] distribution in the FS, with 50 kW heat load and 0.25 kg/s mass flow (deformed shape amplified x200)

1/6 pp

Tables

	Water flow [kg/s]	Water velocity [m/s]	Inner wall temp [°C]	Water outlet temp [°C]	Press drop [bar]
FARADAY SHIELD					
3x1 mm ² (30 kW)	0.25	4.7	47.5	48.7	1.9
3x1 mm ² (60 kW)	0.25	4.7	71	77.4	1.9
4x1.4 mm ² (60 kW)	0.4	4	60	55.8	1.0
RF COILS					
High flow	0.05	4	33.6	43.9	7
Low flow	0.025	2	46.4	67.8	1.8
SOURCE CASE					
Lateral wall	3.2	3.5	30.5	23.5	0.25
Drivers plate	0.4	3.7	57.4	58.7	2.6

Table 1 Main results of the preliminary analytical evaluations

1/6 pp

Cross Section	Water flow	Water velocity	Pressure drop in channels	Water outlet temp	Max temp in copper	Max equiv stress
	[kg/s]	[m/s]	[MPa]	[°C]	[°C]	[MPa]
3x1	0.25	4.66	0.15	67.8	91.2	99.7
3x1	0.275	5.15	0.18	63.5	86.8	92.6
3x1	0.30	5.61	0.20	59.8	83.0	86.6
3x1	0.325	6.07	0.24	56.8	79.8	81.4
4x1.4	0.25	2.49	0.03	67.1	99.6	87.1
4x1.4	0.275	2.75	0.037	62.9	94.8	82.4
4x1.4	0.30	3	0.043	59.2	91.2	77.7
4x1.4	0.325	3.24	0.05	56.2	87.1	73

Table 2 Results of the water flow sensitivity analysis (total heat load = 50 kW)

1/2 pp